INTERNATIONAL JOURNAL OF REFRIGERATION 35 (2012) 2332–2338

Available online at www.sciencedirect.com

SciVerse ScienceDirect

journal homepage: www.elsevier.com/locate/ijrefrig

Study of mass flow distribution between stages in a two-stage pulse tube cryocooler capable of 1.1 W at 4.2 K

L.M. Qiu, K.H. Zhang, W.Q. Dong, Z.H. Gan, C. Wang, X.J. Zhang*

Institute of Refrigeration and Cryogenics, Zhejiang University, Hangzhou 310027, PR China

A R T I C L E I N F O

Article history:
Received 14 February 2012
Received in revised form
6 July 2012
Accepted 15 July 2012
Available online 25 July 2012

Keywords:
Pulse tube cryocooler
Mass flow rate
Cooling power
REGEN

A B S T R A C T

The mass flow distribution among stages is important for design and optimization of multi-stage cryocoolers, which has been seldom investigated due to the complicated mutual interference among stages. The cooling performance's dependence on operating parameters was investigated in a home-made separate two-stage pulse tube cryocooler (PTC), in which mass flow to each stage can be conveniently adjusted. The numerical study revealed the dependence of cooling performance of the second stage on mass flow rate and precooling temperatures. The experiments with different mass flow rates were performed and results agreed well with simulation. Cooling power of 0.7 W at 4.2 K was obtained with single-compressor and mass flow rate of 3 g s^{-1} on the second stage; in the two-compressor driving mode, 1.1 W at 4.2 K was achieved with input power of 11.7 kW, which is the largest cooling power ever obtained at liquid helium temperatures in a separate PTC.

Etude sur la répartition du débit massique entre les étages d'un cryorefroidisseur biétagé à tube à pulsation d'une puissance de 1,1 W à 4,2 K

Mots clés : Cryorefroidisseur à tube à pulsation ; Débit massique ; Puissance frigorifique ; REGEN

1. Introduction

It is now well accepted to employ a multi-stage cryocooler to supply cooling power at different cryogenic temperatures simultaneously in practical applications. For example, a multi-stage cryocooler used in MRI (Magnetic Resonance Imaging) system supplies the precooling at 40–50 K for radiation shields in the first stage, as well as cooling for magnets at liquid helium temperatures in the second stage. Intrinsically, the mass flow has significant effects on the cooling performance of the cryocooler (Wang, 1997). However, due to the difficulties in accurate measurement of mass flow rate in oscillating flow at low temperatures, and the mutual interference among stages, there is few quantitative research to accurately investigate the relationship between the mass flow distribution and cooling performance. The optimal distribution of mass flow among stages is still challenging to be determined for a multi-stage cryocooler (Radebaugh, 1999).

* *Corresponding author*. Tel./fax: +86 571 87952793.
E-mail addresses: Limin.Qiu@zju.edu.cn (L.M. Qiu), Xuejzhang@zju.edu.cn (X.J. Zhang).
0140-7007/$ – see front matter
http://dx.doi.org/10.1016/j.ijrefrig.2012.07.006

Nomenclature

m	mass, kg
Cp	heat capacity of gas at constant pressure, kJ kg^{-1} K^{-1}
Q_1	cooling power at 1st stage, W
Q_2	cooling power at 2nd stage, W
T_1	temperature of first stage, K
T_2	temperature of second stage, K
f	operating frequency, Hz
θ	phase angle
η_E	exergy efficiency
P_0	average pressure, MPa
ε	performance coefficient of pulse tube
$\dot{m}_h$	mass flow rate at the hot end, g s^{-1}
$\dot{m}_c$	mass flow rate at the cold end, g s^{-1}
Subscripts	
R	Regenerator
E	Exergy

Compared to the traditional regenerative cryocoolers, pulse tube cryocoolers have advantages of low vibration, long meantime between maintenance (MTBM) and low electromagnetic interference (EMI) with the absence of the moving parts at cryogenic temperatures (Radebaugh, 2003; Wang, 2008; Ross, 2007). There are mainly two structures: the coupled type (Wang et al., 1997; Chen et al., 1997; Qiu and Thummes, 2002; Qiu et al., 2001) (also termed gas-coupled) and the separate type (Jiang et al., 2004; Zhu et al., 2003; Qiu et al., 2005) (also called thermally coupled). The essential difference between the two types is the precooling method for the working fluid of the low temperature stage. In a coupled type two-stage PTC the working fluid shares the same gas channels in the first stage regenerator, while for the separate type the gas in the second stage is separate and precooled by the heat conductance through a thermal link from the cold end of the first stage. Up to now, most research has focused on coupled type PTCs mainly for the compact structure, even though one has to deal with complicated mutual interference of flow and heat transfer between two stages. Besides, due to the difficulties in accurate measurement, it is hard to optimize the distribution of mass flow for a coupled type PTC. However, one can possibly detect the relationships between the mass flow rate and operating conditions independently for each stage in a separate PTC to obtain the optimal cooling performance (Jiang et al., 2004).

In this study, a separate two-stage PTC was employed to investigate the optimization of mass flow distribution among stages with a large range of precooling temperature and difference driving modes. Based on the simulation results, the experiments with different mass flow rates of the second stage were carried out, in an effort to improve multi-stage PTC design and optimization.

2. Simulation results

The NIST program, Known as REGEN (Gary and Radebaugh, 1991) is used for regenerator simulation (Radebaugh and Gallagher, 2006; Nguyen et al., 2004). It has been successfully

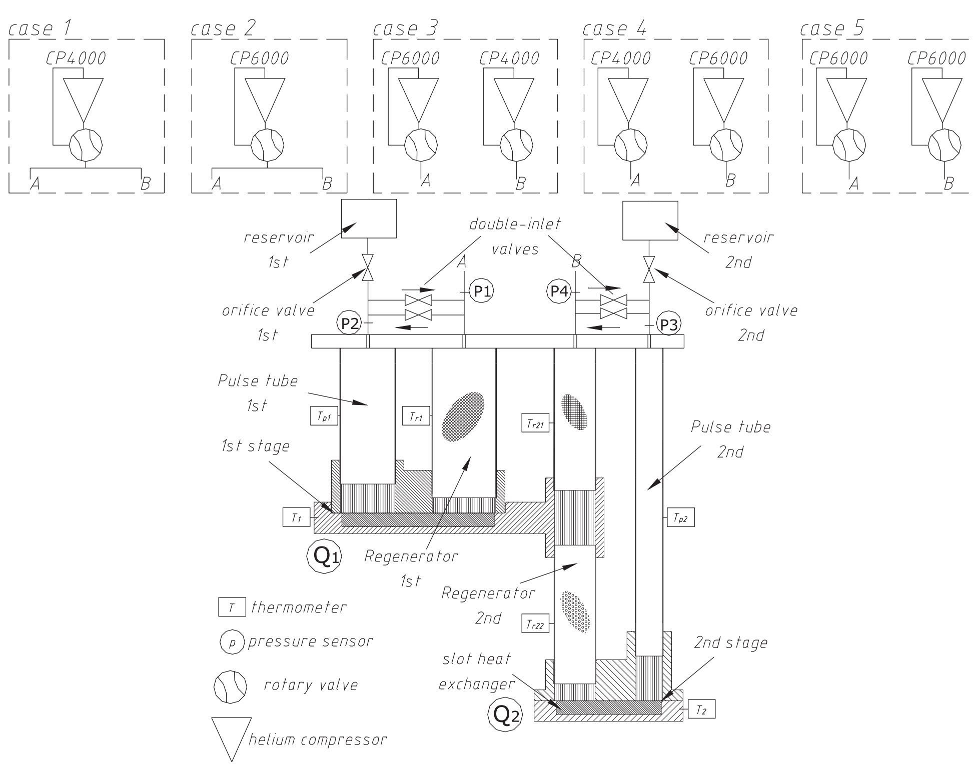

Fig. 1 – Schematic of the separate two-stage PTC with different driving modes.

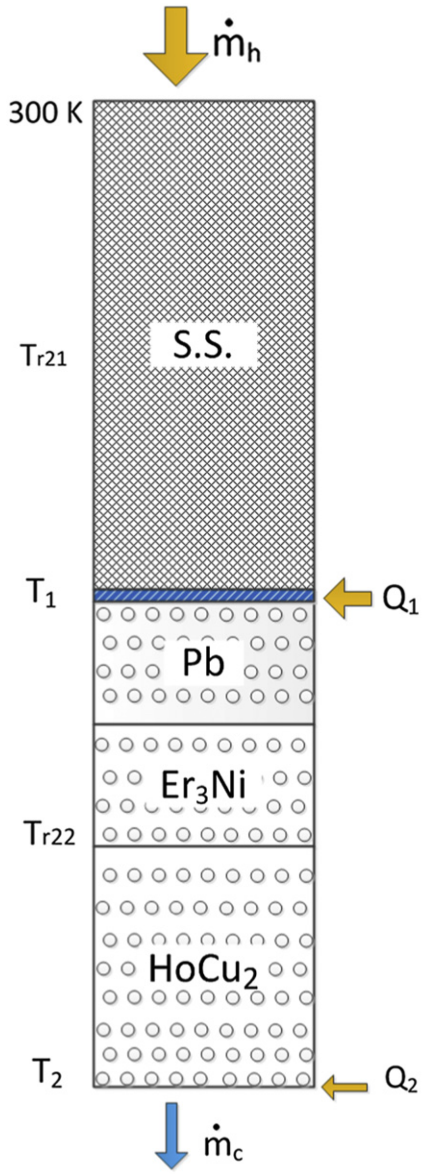

Fig. 2 – Schematic of the second stage regenerator used in REGEN simulation.

applied in the simulation of single stage G-M type PTC (Gan et al., 2009) and 4 K G-M cryocooler (Radebaugh et al., 2002). The regenerator model considered in REGEN is a tube filled with a porous medium. An oscillatory flow of helium passes through the void space in the porous medium and exchanges heat with the regenerative materials. The model is based on the numerical solution of one-dimensional equations for the flow of the helium through the porous matrix with an additional thermal conservation equation for the temperature of the matrix (Gary and Radebaugh, 1991).

This study focused on a separate two-stage PTC with different driving modes, a schematic of the system is displayed in Fig. 1. To simplify the simulation, a numerical analysis with the software REGEN 3.3 was applied to simulate the performance of the second stage regenerator, where lead spheres and magnetic regenerative materials were packed, as shown in Fig. 2. Table 1 shows the main parameters, including regenerator geometry and matrix structure for simulation.

2.1. *Calculation results with different mass flow rates of the second stage*

Fig. 3 illustrates the cooling power's dependence on the mass flow rate of the second stage at 4.2 K with variation of precooling temperature (T_1). The cooling power increases sharply with the mass flow rate increase from 3 to 5 g s^{-1}. The second stage cooling performance is unaffected by the precooling temperature, which was also experimentally verified by Wang (Wang and Gifford, 2002). However, as the mass flow rate rises above 5 gs^{-1}, the slope of the regenerator loss becomes larger, which includes heat transfer loss caused by heat transfer temperature differences, and pressure drop loss caused by flowing resistance and void volume, especially when the precooling temperature is higher than 40 K, see Fig. 4. Due to the increasing regenerator loss, the rise of the cooling power decelerates with the precooling temperature below 40 K. When the precooling temperature is higher than 40 K, the cooling power at 4.2 K significantly decreases.

Fig. 5 shows the heat capacity ratio's dependence on the second stage mass flow rate. $m_{He}Cp_{He}$ and $m_R Cp_R$ are the heat capacity of helium and regenerator matrix respectively. The regenerator loss is mainly determined by the mass flow rate

Table 1 – Matrix and operating parameters of regenerator.

2nd stage regenerator (Ø 30 mm × 0.3 mm × 347.6 mm)	Warm part of the regenerator (temperature range: T_1–300 K)	#247 mesh stainless steel screen (length of 173 mm)
	Cold part of the regenerator (temperature range: 4.2 K-T_1)	Pb spheres with diameter of 0.25 mm (length: 43 mm)
		Er_3Ni spheres with diameter of 0.25 mm (length: 43 mm)
		$HoCu_2$spheres with diameter of 0.25 mm (length: 87 mm)
Hot end temperature, T_1 (K)		20–60
Cold end temperature, T_2 (K)		2.8–4.2
Frequency, f (Hz)		1.1–1.6
Mass flow rate at the hot end, $\dot{m}_h$ (g s^{-1})		3–11
Phase angle (mass flow at the cold end leading the pressure) θ		0°
Average pressure, p_0 (MPa) (abs.)		1.7
Pressure ratio at the cold end ($f = 1.3$ Hz)		1.9
Performance coefficient of pulse tube, ε		0.9

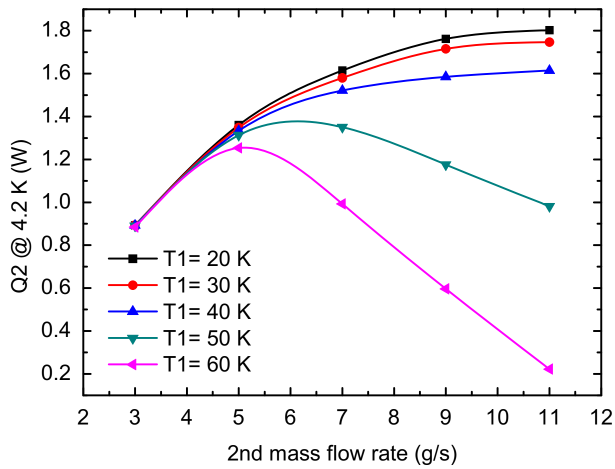

Fig. 3 – Calculated cooling power at 4.2 K with different mass flow rates.

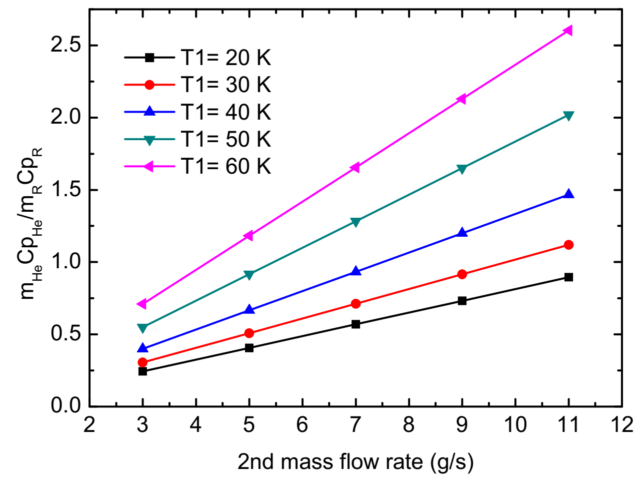

Fig. 5 – Heat capacity ratio's dependence on the second stage mass flow rate.

with the fixed diameter. The heat capacity of helium significantly increases with precooling temperature and second stage mass flow rate. The regenerator loss increases because of the limited regenerative capacity, when the mass flow rate is higher than 5 g s^{-1}. The precooling temperature has small effect on the regenerator loss, which is nearly the same as the precooling temperature is below 40 K. The mass flow rate in the second stage should be optimized for the highest efficiency.

2.2. *Mass flow distribution among stages of two-stage PTC*

Fig. 6 shows the precooling power's dependence on the second stage mass flow rate. The precooling power decreases with the rise of the precooling temperature. The second stage mass flow rate varies from 2.5 to 3.5 g s^{-1} with the precooling temperature varying from 25 to 40 K. The average mass flow rate of 3 g s^{-1} is considered in the second stage. About 37.5% of the total mass flow enters the second stage and the rest enters the first stage with the precooling temperature varying from 25 to 40 K in a two-stage PTC.

3. Experimental setup

Fig. 1 shows the schematic of the separate two-stage PTC (G-M type) used in this study, and the experimental apparatus with two compressors driven is displayed in Fig. 7. The first stage and second stage are thermally coupled. The pulse tubes and regenerators are fabricated from stainless steel tubes with outer diameter, wall thickness and length as follows: 1st stage regenerator: 46.6 mm × 0.5 mm × 205.6 mm; 1st stage pulse tube: 40.6 mm × 0.5 mm × 195.5 mm; 2nd stage regenerator: 30 mm × 0.5 mm × 347.6 mm; 2nd stage pulse tube: 20 mm × 0.3 mm × 367.3 mm. The cryocooler operated in double-inlet mode with anti-parallel arrangement to adjust the DC flow. Water-cooled helium compressors of Leybold CP6000 and CP4000 were used with rated input power of 6 kW and 4 kW. The cryocooler could be driven by two compressors together with two rotary valves. The mass flow rates were approx. 8 g s^{-1} and 5 g s^{-1}, respectively (data from the compressor user

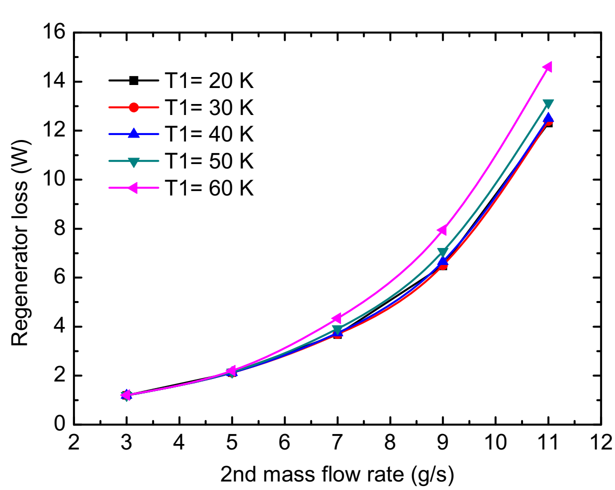

Fig. 4 – Calculated regenerator loss with different mass flow rates.

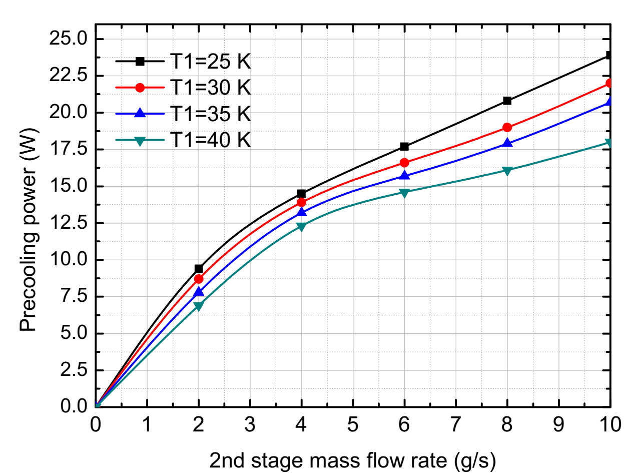

Fig. 6 – Precooling power's dependence on the second stage mass flow rate.

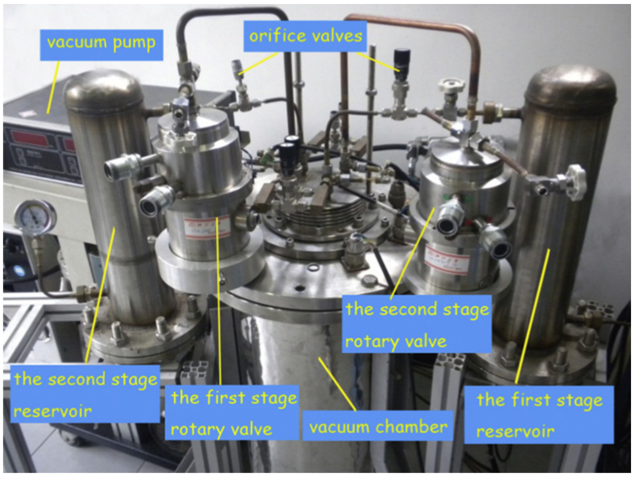

Fig. 7 – Photograph of experimental apparatus of separate two-stage PTC in two-compressor driven modes Case 3–5.

manual). The refrigeration temperatures of both stages (T_2, T_2) were measured by calibrated Rh–Fe resistance thermometers with an accuracy of 0.1 K. The cooling power was determined by measuring the electrical power input to a heater tightly attached to the cold end with an accuracy of 1.0 mW. Calibrated Pt100 resistance temperature sensors were installed on the outer wall of pulse tubes and regenerators to monitor the temperature distributions for both stages.

4. Experimental results

In order to verify the above simulation results, the experiments manipulating mass flow rate levels in the second stage were carried out. Table 2 lists the driving modes for the two-stage PTC. A single compressor was used in Case 1 and Case 2. Two compressors were used in Case 3, Case 4 and Case 5.

Figs. 8 and 9 display the cooling power's dependence of the second stage in relation to the different driving modes. The mass flow rate plays a dominant role in the cooling performance as predicted. According to the increasing mass flow rate of the second stage varied from Case 1 to Case 4, the cooling performance of the second stage rises. Considering Case 4 and Case 5, the cooling performance is nearly the same with the same compressor driven in the second stage, though the mass flow rate increases at the first stage from Case 4 to Case 5. Comparing Fig. 8 ($Q_1 = 0$ W) with Fig. 9 ($Q_1 = 20$ W), the tendencies of cooling performance of the second stage are nearly the same. Contrast to the mass flow rate, the extra heat load of the first stage has slight effect on the cooling performance of the second stage. The optimal cooling performance was achieved when the first stage was driven by CP4000 and the second stage was driven by CP6000 (Case 4). Cooling power of 1.1 W at 4.2 K was obtained with a total input power of 11.7 kW. It is estimated that if the two stages are both driven by CP4000 compressors, the cooling power of 1.0 W at 4.2 K could be achieved with a total input power within 10 kW.

It is necessary to evaluate the efficiency for the two-stage PTC, when it supplies cooling power at different temperatures simultaneously. Exergy efficiency η_E (Qiu and Thummes, 2001), instead of conventional COP (coefficient of performance), was used to evaluate the performance, which is listed in Table 2. The exergy efficiency of the two-compressor driving mode (Case 3, Case 4 and Case 5) was much lower than that of the single-compressor driving mode because of the large regenerator losses of the second stage. This is because the present diameter of the second stage regenerator was inadequate for the high mass flow rate of two-compressor driven modes. In effect, the regenerative capacity was insufficient.

Fig. 10 shows the typical load map of the 4 K PTC with two compressors and two rotary valves (Case 4). The first stage was driven by compressor CP4000 and the second stage was driven by CP6000, respectively. The hot end mass flow rate of the second stage was about 8 g s^{-1}. The working frequency of the two stages was 1.3 Hz, the same as the single-compressor driving mode. The average pressure of the second stage was 1.7 MPa and the lowest refrigeration temperature was 2.3 K. The cryocooler can provide 1.1 W at 4.2 K and 10 W at 40 K simultaneously. The cooling performance of the second stage was better than the single-compressor driving mode because of the larger mass flow rate. However, the precooling power to the second stage regenerator was also much higher. The first stage cooling power was 10 W lower compared to the single-compressor driving mode.

Fig. 11 shows the comparison of cooling power at 4.2 K with different mass flow rates in the second stage. The simulation results agree with the experimental results in tendency. Actually, the regenerator losses in the experiment were higher than the calculated, especially under the condition of high mass flow, mainly due to some losses (e.g. conduction loss, nonideal heat exchange loss etc.) not considered in the model.

Fig. 12 shows the comparison of cooling power with different refrigeration temperatures. The first stage and second stage were driven by CP4000 and CP6000 respectively

Table 2 – Driving modes for the separate pulse tube cryocooler.

Driving mode	Compressor[a]		Mass flow rate (g s^{-1})		Total actual power consumption (kW)	Exergy efficiency (%)
	1st stage	2nd stage	1st stage	2nd stage		
Case 1	CP4000		3.0	2.0	4.8	2.83
Case 2	CP6000		5.0	3.0	6.9	2.60
Case 3	CP6000	CP4000	8.0	5.0	11.7	1.62
Case 4	CP4000	CP6000	5.0	8.0	11.7	1.56
Case 5	CP6000	CP6000	8.0	8.0	13.8	1.50

a Rated input power: CP4000 – 4.0 kW; CP6000 – 6.0 kW.

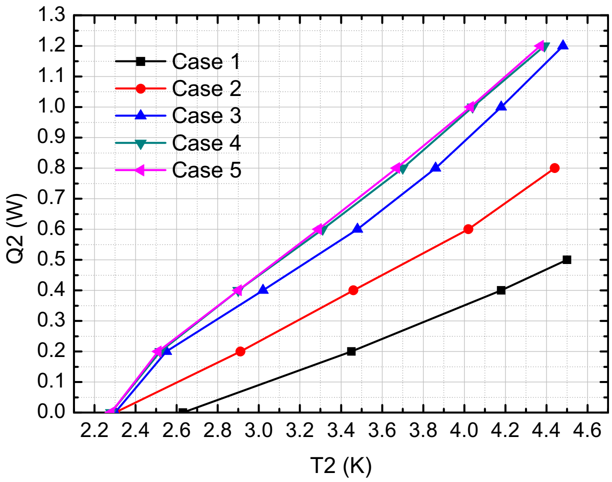

Fig. 8 – Comparison of cooling power's dependence on the different driving mode with Q1 = 0 W.

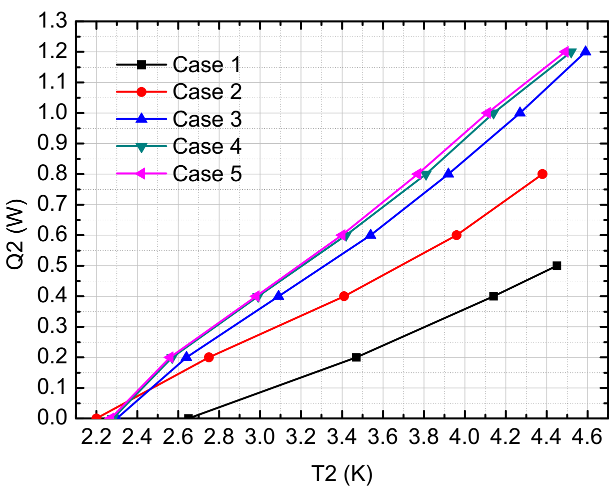

Fig. 9 – Comparison of cooling power's dependence on the different driving mode with Q1 = 20 W.

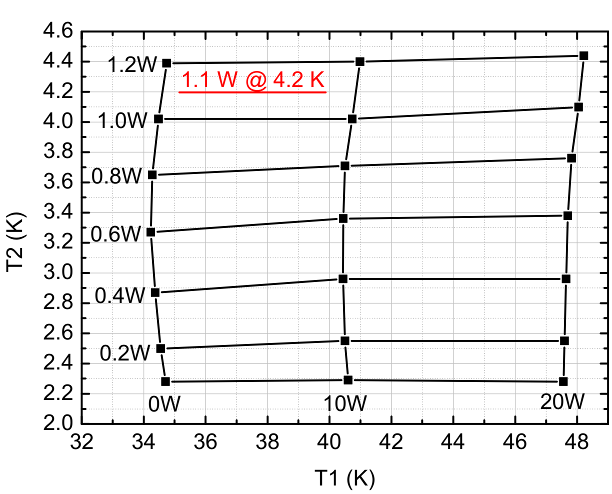

Fig. 10 – Load map of the 4 K PTC with two compressors and rotary valves (Case 4).

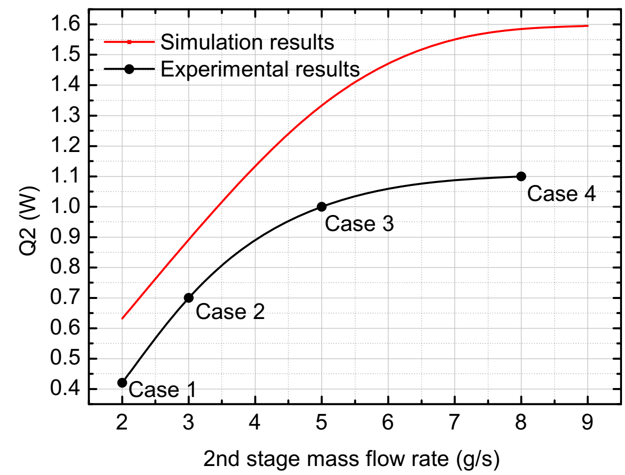

Fig. 11 – Comparison of cooling power with different mass flow rates at the second stage.

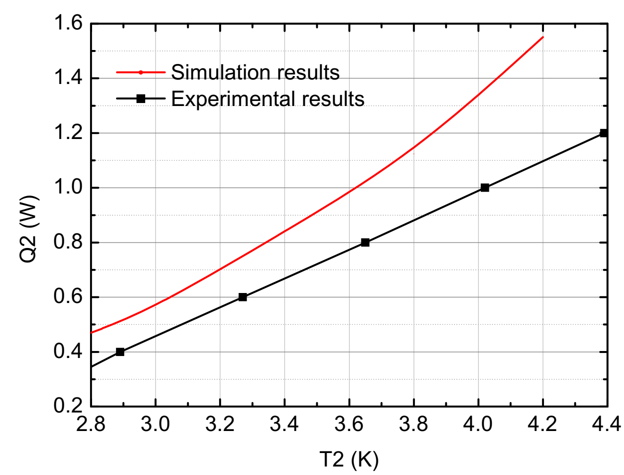

Fig. 12 – Comparison of cooling power with different refrigeration temperature.

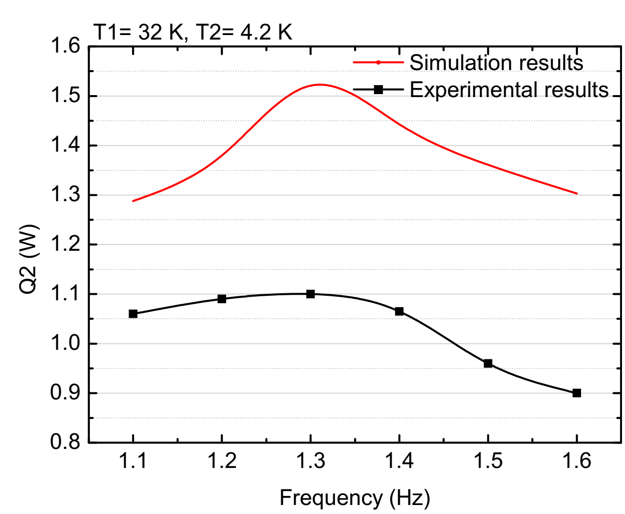

Fig. 13 – Dependence of cooling performance on operating frequency.

(Case 4). The mass flow rate of the second stage was 8 g s^{-1} in the simulation. The slopes of the two cooling power curves (dQ/dT) are nearly the same especially below 4 K. Fig. 13 shows the cooling performance dependence on the operating frequency. The experimental results are in accordance with the calculation results. The optimal frequency is 1.3 Hz for the second stage, which is the same as the experiments.

5. Conclusions

The distribution of mass flow among stages plays an essential role in multi-stage PTCs. Dependence of cooling performance of the second stage on mass flow rate and precooling temperature was quantitatively revealed based on the simulation with REGEN. About 37.5% of the total mass flow rate enters the second stage and the rest enters the first stage with the precooling temperatures from 25 to 40 K. As increase of mass flow rate in the second stage, regenerator loss (mainly caused by inefficient loss and pressure drop) sharply rises, and there is an optimal cooling capacity of the second stage. The experiments with different mass flow rates in the second stage were carried out. Cooling power of 0.7 W at 4.2 K and 20 W at 40 K were achieved simultaneously with a single compressor and the mass flow rate of the second stage was 3 g s^{-1}. Two compressors together with rotary valves were used to drive the two stages respectively and the cryocooler can provide 1.1 W at 4.2 K and 10 W at 40 K with the second stage mass flow rate of 8 g s^{-1}, which is the largest cooling power ever obtained in a separate 4 K PTC. The total actual input power was 11.7 kW.

Acknowledgements

The project is supported by National Funds for Distinguished Young Scientists of China under Contract NO. 50825601 and partly by the Major State Basic Research Development Program of China under Contract NO. 2011CB706501.

REFERENCES

Chen, G.B., Qiu, L.M., Zhen, J.Y., 1997. Experimental study on a double-orifice two-stage below 4 K. Cryogenics 37, 271–273.

Gary, J., Radebaugh, R., 1991. An improved model for the calculation of regenerator performance (REGEN 3.1). In: Proc. Fourth Interagency Meeting on Cryocoolers, David Taylow Research Center Technical Report DTRC91/003, 165–176.

Gan, Z.H., Dong, W.Q., Qiu, L.M., et al., 2009. A single-stage GM-type pulse tube cryocooler operating at 10.6 K. Cryogenics 49, 198–201.

Jiang, N., Lindemann, U., Giebeler, F., 2004. A 3He pulse tube cooler operating down to 1.3 K. Cryogenics 44, 809–816.

Nguyen, C., Yechley, A., Culler, A., et al., 2004. Hydrogen/oxygen propellant densifier using a two-stage pulse tube cryocooler. In: Waynert, J., et al. (Eds.), Advances in Cryogenic Engineering 49B. Plenum Press, New York, pp. 1703–1709.

Qiu, L.M., Naumazawa, T., Thummes, G., 2001. Performance improvement of a pulse tube cooler below 4 K by use of GdAlO3 regenerator material. Cryogenics 41, 693–696.

Qiu, L.M., Thummes, G., 2001. Two-stage pulse tube cooler for operation of a Josephson voltage standard near 4 K. Adv. Cryogenic Eng. 47, 625–632.

Qiu, L.M., Thummes, G., 2002. Valve timing effect on the cooling performance of a 4 K pulse tube cooler. Cryogenics 42, 327–333.

Qiu, L.M., He, Y.L., Gan, Z.H., et al., 2005. A separate two-stage pulse tube cooler working at liquid helium temperature. Chin. Sci. Bull. 50, 1030–1033.

Radebaugh, R., 1999. Development of the pulse tube refrigerator as an efficient and reliable cryocooler. Proc. Inst. Refrigeration 96, 11–31.

Radebaugh, R., Gallagher, A.O., Gary, J., 2002. Regenerator behavior at 4 K: effect of volume and porosity. Adv. Cryogenic Eng. 47, 961–968.

Radebaugh, R., 2003. The development and application of cryocoolers since 1985. In: Chen, G.B., Hebral, B., Chen, G.M. (Eds.), Proceedings of ICCR'2003. International Academic Publishers/Beijing World Publishing Corporation, pp. 858–870.

Radebaugh, R., Gallagher, A.O., 2006. Regenerator operation at very high frequencies for microcryocoolers. In: Weisend, J.G., et al. (Eds.), Advances in Cryogenic Engineering 51B. Plenum Press, New York, pp. 1919–1928.

Ross, R.G., 2007. An Overview of NASA Space Cryocooler Programs-2006. Cryocooler 14. ICC Press, Boulder, Colorado, pp. 1–10.

Wang, C., 1997. Numerical analysis of 4 K pulse tube cooler: Part II. Performances and internal processes. Cryogenics 37, 215–220.

Wang, C., Thummes, G., Heiden, C., 1997. A two-stage pulse tube cooler operating below 4 K. Cryogenics 37, 159–164.

Wang, C., Gifford, P.E., 2002. Development of 4 K pulse tube cryorefrigerators at Cryomech. In: Susan Breon, et al. (Eds.), Advances in Cryogenic Engineering, vol. 47. Plenum Press, New York, pp. 641–648.

Wang, C., 2008. Development and application of low frequency pulse tube cryocooler. In: Cryogenics and Proceedings of International Conference of Cryogenics and Refrigeration (ICCR)'2008, pp. 61–70.

Zhu, S.W., Nogawa, M., Katsuragawa, S., et al., 2003. Performance of a 4 K Pulse Tube Refrigerator and its Improvement. Cryocooler 12. Plenum Press, New York, pp. 309–315.